IEEE Access
Multidisciplinary | Rapid Review | Open Access Journal

Received 1 August 2023, accepted 22 August 2023, date of publication 30 August 2023, date of current version 6 September 2023.

Digital Object Identifier 10.1109/ACCESS.2023.3310247

METHODS

Improved SIC-SVD Hybrid Precoding Algorithm for Indoor Sub-THz Systems

HANG GUI[1], YUANYUAN XIE[1], QINGHENG SONG[2], YINGJING QIAN[2], AND RENMIN ZHANG[1,2], (Member, IEEE)

[1]School of Communication and Electronic Engineering, Jishou University, Jishou 416000, China
[2]Key Laboratory of Intelligent Control Technology for Wuling-Mountain Ecological Agriculture in Hunan Province, Huaihua University, Huaihua, Hunan 418000, China

Corresponding authors: Yingjing Qian (Qyingjing@163.com) and Renmin Zhang (rzhang1981@163.com)

This work was supported in part by the National Natural Science Foundation of China under Grant 62061017; in part by the NSF of Hunan Province under Grant 2021JJ30556, Grant 2021JJ30545, and Grant 2022JJ50310; in part by the Education Commission of Hunan Province under Grant 22B0761 and Grant 2020JGZD064; in part by the Fund of Central Support for Local Science and Technology Development under Grant 2022ZYC012; in part by the Project of Hunan Provincial Enterprise Science and Technology Commissioner under Grant 2021GK5096; and in part by the Postgraduate Innovation Base Open Projects of Jishou University under Grant XXJD202202.

ABSTRACT Emerging terahertz (THz) communication will become the main way of wireless communication in the future, it will also use hybrid precoding which combines analog and digital hybrid precoding like millimeter wave communication systems, to reduce the system energy consumption. Indoor as a main scenario for communication, to better meet the demands for data transmission. In this paper, an improved hybrid precoding method based on successive interference cancelation and singular value decomposition (SIC-SVD) is proposed for indoor Sub-THz communication system with sub-connected structures. However, the introduction of phase shifters imposes constant modulus constraints, making the problem of hybrid precoding difficult to solve directly. The proposed method first decomposes the optimization problem of achievable rates for the system, based on the special structure of sub-connected, into a series of equivalent sub-problems. The algorithm first designs the analog precoding matrix according to the SIC method, after obtaining the designed analog precoding matrix, the algorithm defines an equivalent channel and employs singular value decomposition (SVD) to obtain the digital precoding matrix. The simulation results show that compared with the existing method based on SIC, the proposed algorithm has slightly higher achievable rate and is closer to the optimal full-digital precoding method. At the same time, this paper also presents a simple analysis of the proposed algorithm for imperfect channel state information (CSI) with different accuracy. Simulation results show that the spectral efficiency is also very near to the perfect CSI case when the accuracy of the CSI is 0.9.

INDEX TERMS Sub-THz, indoor communication, hybrid precoding, SIC.

I. INTRODUCTION

With the rapid development of information age, the capacity demand of wireless communication is also growing rapidly [1], [2]. The millimeter-wave band (30-300GHz) can no longer meet the needs of communication equipment and techology. In order to alleviate the shortage of spectrum resources and meet the rapid growth of wireless data rates, it is inevitable to explore new frequency bands. The terahertz band has the advantage of a larger available bandwidth than the millimeter-wave band, with more than ten times the frequency increase [3], [4]. At the same time, the terahertz frequency band (0.1-10THz) is considered as a primary frequency band for 6G wireless communication [5], due to offering abundant spectrum resources and addressing the issues of spectrum shortage and capacity limitation effectively in wireless communication systems [6], [7]. Furthermore, the significantly decrease in wavelength allows for more antennas to compensate for severe path loss through precoding techniques, providing more antenna gains and spatial diversity gains to communication systems, it is also considered as a promising candidate for indoor communication due to its enormous spectrum availability and feasibility of combating severe propagation attenuation and interference

The associate editor coordinating the review of this manuscript and approving it for publication was Hasan S. Mir.

with large-scale antenna arrays. The indoor scenario is a common communication environment in our daily life [8], [9], [10]. For example, markets, gyms, office buildings and other indoor occasions.When signals are transmitted in the aforementioned indoor environment, they will be prone to interferences, which will limits the performance of communication system. We can reduce interference and send signal in a specific direction by precoding [11]. Therefore, it is necessary to design a hybrid precoding method to obtain antenna array gains for indoor wireless communication scenarios.

In present millimeter and terahertz-wave communication systems, considering the system power consumption and complexity, traditional digital/analog precoding is no longer applicable, thus hybrid precoding structure [12] has been proposed by related scholars. This novel structure has attracted a lot of attention due to its advantage of having fewer RF chains than the transmitter antennas and has been successfully used in millimeter wave multiple-input multilpe-output (MIMO) communication systems to reduce hardware cost and complexity. At the same time, the antenna structure of the transceiver is a key techology that affects the communication performance. Most of previous relevant precoding works are based on fully-connected structure, where each RF chain is connected to each antenna via phase shifter for signal transmission; theoretically, fully-connected structure is closest to the communication system optimal performance. In [13], a precoding vector has been designed for the transmitter by utilizing the sparsity of the received signal with fully-connected structure. For multi-user communication system with fully-connected structure, [14] designs analog matrix by extracting the conjugate transposed phase information of the channel. The digital part is obtained through block diagonalization and zero-forcing design of the equivalent channel matrix, which reduces the matrix dimension and hardware complexity. However, as the frequency increases, the number of antennas at the transceiver also increases, making it difficult to load the hardware and system power required for fully-connected structure. Therefore, another traditional structure is proposed: sub-connected structure [15]. Different from fully-connected structure, sub-connected structure, a RF chain is only connected to a subarray composed of some antennas, so the number of RF chains and phase shifters have been greatly reduced, achieving a good balance between system cost and performance. Hence, the research on hybrid precoding methods for sub-connected structures has been attracted widespread interest from experts and academics. A hybrid precoding method for sub-connected structure was first proposed and designed in [16], which sequentially designs the precoding matrix at the transmitter based on the block diagonalization characteristics of precoding matrix. However, the method pre-designed the digital precoding matrix as a diagonal matrix, which leads to a loss of generality in digital precoding. Additionally, the gains of this method are solely derived from the analog precoding part, resulting in a partial performance degradation.

In addition, the higher frequency and shorter wavelength of sub-THz signals enables a large number of antennas to be place in a very small footprint, the basic component becomes a subarray instead of an antenna, and no longer provides dedicated RF chain for a antenna. Considering the complexity of circuits and cost in sub-THz communication system. It is more suitable to deploy the sub-connected structure for sub-THz systems.

Based on the aforementioned scenarios and existing problems, inspired by the successive interference cancelation (SIC) -based hybrid precoding method in MIMO point-to-point systems, this paper proposed an improved hybrid precoding algorithm based on successive interference cancelation and singular value decomposition, built upon its method and sub-connected structure used for hybrid precoding. The main contributions of this article are as follows:

1) In this paper, for the indoor sub-THz communication system, the Access Point (AP) uses efficient sub-connected structure. In order to better elimimate interference between different subarrays. According to the specific sub-connected structure at AP, the system total rate optimization problem can be decomposed into sub-rate optimization problems of multiple sub-antenna arrays.

2) Specifically, for different sub-antenna arrays, to eliminate interference and compensate for transmission loss. We propose an improved precoding method, according to the method of successive interference cancelation in [16], design the analog precoding vector for the first sub-antenna array based on corresponding rate optimization sub-problem, the problem can transform into sequentially designing analog precoding vectors by minimizing the mean square error (MSE) between unconstrained optimal analog precoding vectors and designing analog precoding vectors; after the part of first sub-antenna array is eliminated from the expression of total achievable rate, then design the rest of sub-antenna arrays in the same way. Next, according to the equivalent channel matrix formed by channel matrix and the designed analog precoding matrix. We use the traditional singular value decomposition (SVD) method to design the digital precoding matrix for equivalent channel matrix.

3) The final analysis and simulation results verify that the performance and effectiveness of proposed hybrid preocding method is slightly better than the method of literature [16], and it is very close to the desired optimal unconstrained precoding achievable rate. At the same time, the results in imperfect channel state information (CSI) cases are also considered, and the proposed algorithm demonstrates excellent performance and robustness.

The rest of this paper is organized as follows. Section II briefly described the system model of indoor sub-THz communication system and analyzed the system rate optimation problem. Section III described the decomposition process of optimization problem and the proposed hybrid precoding method based on successive interference cancelation and

singular value decomposition (SIC-SVD). The simulation results of the achievable rate are shown in Section IV. Finally, conclusions are given in Section V.

Notation: In this paper, we will use the following notation:Uppercase boldface letters represent matrices and lowercase boldface letters denote vectors. $(.)^T$, $(.)^H$, $(.)^{-1}$, $|.|$ denote the transpose, conjugate transpose, inversion, and determinatant of a matrix, respectively. $||.||_2$ denote the ℓ_2-norm of a vector. $\mathrm{Re}\{.\}$ and $\mathrm{Im}\{.\}$ denote the real part and imaginary part of a complex number, respectively; Finally, $\mathbf{I}_N$ is $N \times N$ identity matrix.

II. SYSTEM MODEL AND PROBLEM DESCRIPTION

A. SYSTEM MODEL

This paper mainly study the sub-THz large-scale antennas point to point communication system with sub-connected structure in indoor environment, which can reduce the extensive use of phase shifters, we first assume that the indoor AP and user have perfect CSI. The AP is equipped with N_t antennas and N independent RF chains, the user is equipped with K antennas. Each RF chain derives an individual sub-antenna array with M antennas. The number of sub-antenna arrays is N for sub-connected architecture. To simplify, in this paper, it is assumed that the AP uses N RF chains to transmit N data streams to user with K antennas (i.e. $N = K$). Fig.1 shows a large-scale antenna hybrid precoding point-to-point system model using sub-connected structure [17] in the indoor sub-THz communication environment. The data streams at AP first passes through the baseband for digital precoding, after that, passes through the corresponding N RF chains. Each RF chain is connected to a sub-antenna array with M antennas via M phase shifters [18], analog precoding operation is performed by phase shifters connected to the RF chains before transmission. Since transmitting one data stream requires M phase shifters, to transmit N data streams, sub-connected structure requires NM phase shifters, whereas fully-connected structure requires N^2M phase shifters. The analog precoding part in this paper consists of phase shifters [19], the main characteristics of phase shifters are: different elements have same amplitude, only phases are different. The final transmission signal $\mathbf{x}$ from the data streams by AP after being processed by hybrid precoder can be expressed as:

$$\mathbf{x} = \mathbf{F}_{RF}\mathbf{F}_{BB}\mathbf{s} \tag{1}$$

$\mathbf{s} = [s_1, s_2, \ldots, s_N]^T$ denote the transmitted signal vector in the baseband. We assume used Gaussian signals with normalized signal power $\mathbb{E}(\mathbf{s}\mathbf{s}^H) = \frac{1}{N}\mathbf{I}_N$. After analog and digital precoding, the data streams are sent to user through sub-antenna array connected to the corresponding RF chain, then the signal vector received by user $\mathbf{y} = [y_1, y_2, \ldots, y_K]^T$ in a narrowband system can be presented as

$$\mathbf{y} = \rho\mathbf{H}\mathbf{F}_{RF}\mathbf{F}_{BB}\mathbf{s} + \mathbf{n} = \rho\mathbf{H}\mathbf{F}\mathbf{s} + \mathbf{n}. \tag{2}$$

where ρ is the average power, $\mathbf{F} \in \mathbb{C}^{MN\times N}$ denotes hybrid precoding matrix. $\mathbf{F}_{BB}$ is digital precoding matrix. $\mathbf{F}_{RF}$ is analog precoding matrix. To satisfy the constraint of total transmission power, it is required that $\|\mathbf{F}\|_F \leq N$. The analog matrix under sub-connected structure is as follows:

$$\mathbf{F}_{RF} = \begin{bmatrix} \mathbf{f}_{RF,1} & \mathbf{0} & \cdots & \mathbf{0} \\ \mathbf{0} & \mathbf{f}_{RF,2} & & \mathbf{0} \\ \vdots & & \ddots & \vdots \\ \mathbf{0} & \mathbf{0} & \cdots & \mathbf{f}_{RF,N} \end{bmatrix}_{MN\times N} \tag{3}$$

According to sub-connected structure of the transmit antennas, analog precoding matrix at AP is set as a block diagonalization matrix, facilitating the design of analog precoding vectors for different sub-antenna arrays. $\mathbf{f}_{RF,n} \in \mathbb{C}^{M\times 1}$ is the analog precoding vector corresponding to the different sub-antenna arrays. $\mathbf{H} \in \mathbb{C}^{K\times MN}$ denotes channel matrix based on an indoor sub-THz point to point communication system. $\mathbf{n}$ is an Additive White Gaussian Noise (AWGN) vector, whose entries follow the independent and identical distribution (i.i.d.): $\mathcal{CN}(0, \sigma^2)$.

For the sub-THz indoor channels, sub-THz signals experience more severe path loss and atmospheric attenuation. As a result, the paths generally consist of a LOS ray and several non-LOS (NLOS) rays, the power of LOS path is often stronger than NLOS paths [20]. Because of the stable indoor communication environment and channel transmission conditions, sparse path in sub-THz band, the scattering path is limited [21], and the channel no longer follows the conventional Rayleigh fading. In this article, we adopt common Saleh-Valenzuela (S-V) geometric channel model to reflect characteristics of sub-THz communication system. Therefore, the channel matrix from AP to user can be expressed as [22], [23], and [24]:

$$\begin{aligned} \mathbf{H} &= \mathbf{H}^{LOS} + \mathbf{H}^{NLOS} \\ &= \sqrt{\frac{MN}{L}}\alpha_L \mathbf{a}_{MS}(\theta^r)\mathbf{a}_{AP}^H(\theta^t) \\ &\quad + \sum_{u=1}^{n_{NL}} \alpha_u \mathbf{a}_{MS}(\theta^r)\mathbf{a}_{AP}^H(\theta^t) \end{aligned} \tag{4}$$

where $\sqrt{MN/L}$ is normalization factor. NM is the total number of antennas at AP. n_{NL} is the number of channel NLOS paths, α_u is the gain of u_{th} path, satisfy $\mathcal{CN}(0, 1)$. $\mathbf{a}_{MS}(\theta^r)$ and $\mathbf{a}_{AP}(\theta^t)$ are the antenna array response vectors depending on antenna array structure at AP and user, respectively. θ^t, θ^r are the azimuth angles of departure and arrival (AoDs/AoAs), respectively.

In current research on precoding methods, two commonly used antenna array structures are typically employed: Uniform Linear Array (ULA) and Uniform Planar Array (UPA). This paper considers using ULA structure [25] at transmitter and receiver, and its array structure diagram is shown in Fig.2.

By analyzing and modeling Fig. 2, we can know that the antenna array response vector at AP is [26]:

$$\mathbf{a}^{AP}(\theta) = \frac{1}{\sqrt{MN}}[1, \ldots, e^{jt(\frac{2\pi}{\lambda})D\cos\theta},$$

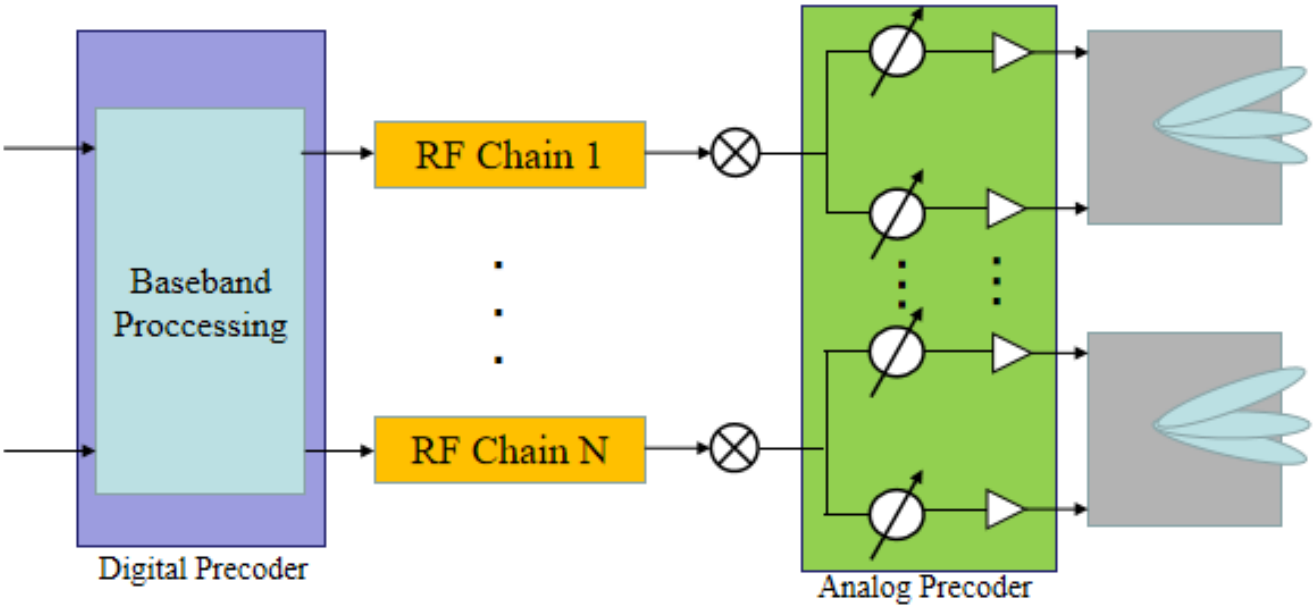

FIGURE 1. Sub-connected architecture of sub-THz systems.

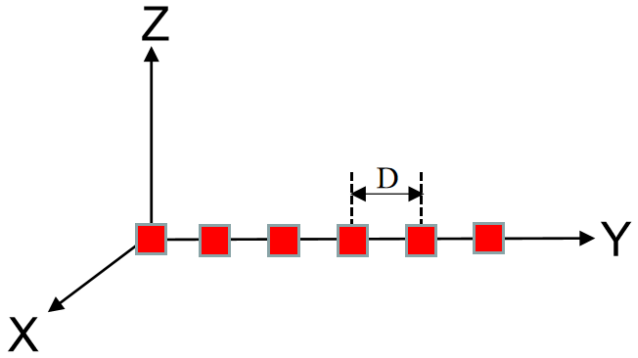

FIGURE 2. ULA array structure.

$$\ldots, e^{j(MN-1)(\frac{2\pi}{\lambda})D\cos\theta}]^T \quad for\ 0 \le t \le (MN-1). \tag{5}$$

The array response vector at receiver has the similar form. λ denotes the wavelength of signal. D is the antenna spacing. In this paper, we assume the knowledge of channel matrix is known perfectly and instantaneously to the AP, which can be obtain by channel estimation with uplink training [27].

B. PROBLEM DESCRIPTION

According to system model and architecture described in Section II-A, since the analog parts of AP is implemented through phase shifters, it will be constrained by the constant modulus of phase shifters. Therefore, the amplitude of each non-zero element in the designed analog precoding matrix is same, only the phase is different.

This article aims to maximize total achievable rate R of the indoor sub-THz point-to-point communication system by designing analog and digital precoders at AP. We only consider the design of precoding matrix at AP and assume perfect decoding at receiver. From Eq.(2), we can know that the expression of the total achievable rate R is:

$$\mathrm{R} = I(\mathbf{s};\mathbf{y}) = \log_2(|\mathbf{I}_K + \frac{\rho}{N\sigma^2}\mathbf{H}\mathbf{F}\mathbf{F}^H\mathbf{H}^H|) \tag{6}$$

The hybrid precoding matrix $\mathbf{F}$ can be expressed as $\mathbf{F} = \mathbf{F}_{RF}\mathbf{F}_{BB}$. In the design procedure, there are some constraints on the design of $\mathbf{F}$:

Constraint 1: As shown in (3), $\mathbf{F}_{RF}$ should be a block diagonalization matrix, i.e. $\mathbf{F}_{RF} = diag[\mathbf{f}_{RF,1}, \mathbf{f}_{RF,2}, \ldots, \mathbf{f}_{RF,N}]$.

Constraint 2: The non-elements in each column of $\mathbf{F}_{RF}$ should have determined amplitude. And the amplitude value is fixed as $1/\sqrt{M}$.

Unfortunately, due to the non-convex constraint of analog precoding matrix $\mathbf{F}_{RF}$, the total achievable rate (6) cannot be directly solved. We can decompose the original communication procedure into two sub-procedures: the analog stage and the digital stage. And this article focus on the design of hybrid beamformer at AP. In this case, we aim to maximize the mutual information $I(\mathbf{s};\mathbf{y})$:

$$\begin{aligned}(\mathbf{F}_{BB}^{opt}, \mathbf{F}_{RF}^{opt}) &= \arg\max_{\mathbf{F}_{BB},\mathbf{F}_{RF}} I(\mathbf{s};\mathbf{y}) \\ &= \arg\max_{\mathbf{F}_{BB},\mathbf{F}_{RF}} \log_2(|\mathbf{I} + \frac{\rho}{N\sigma^2}\mathbf{H}\mathbf{F}_{RF}\mathbf{F}_{BB}\mathbf{F}_{BB}^H\mathbf{F}_{RF}^H\mathbf{H}^H|)\end{aligned} \tag{7}$$

where $\mathbf{F}_{BB}^{opt}$ and $\mathbf{F}_{RF}^{opt}$ are the optimal baseband and analog precoding matrices. The design approach of this article is to calculate $\mathbf{F}_{RF}^{opt}$ at the first step, then derive $\mathbf{F}_{BB}^{opt}$ based on $\mathbf{H}_{eq}$. Let $\mathbf{x}_B = \mathbf{F}_{BB}\mathbf{s}$, the data-processing inequality can be

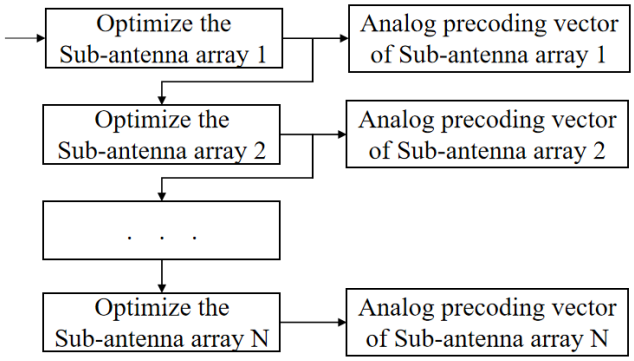

FIGURE 3. Diagram of the SIC analog precoding.

expressed as:

$$I(\mathbf{s};\mathbf{y}) \overset{(a)}{\leq} I(\mathbf{x}_B;\mathbf{y}) \leq C \tag{8}$$

where C represents the capacity of the point-to-point system, famous thin-SVD can let inequality (a) turns into equality. From this, we can infer that $\max I(\mathbf{s};\mathbf{y})$ only depends on the design of $\mathbf{F}_{RF}$. So we have:

$$\begin{aligned}\mathbf{F}_{RF}^{opt} &= \arg\max_{\mathbf{F}_{RF}} I(\mathbf{s};\mathbf{y}) \\ &= \arg\max_{\mathbf{F}_{RF}} \log_2(|\mathbf{I} + \frac{\rho}{N\sigma^2}\mathbf{H}\mathbf{F}_{RF}\mathbf{F}_{RF}^H\mathbf{H}^H|)\end{aligned} \tag{9}$$

At the same time, due to the block diagonalization structure of analog precoding matrix $\mathbf{F}_{RF}$. The approach shown in Fig.3 can be considered in this paper. The sub-connected structure optimization problem with non-convex constraints is decomposed into a series of rate optimization sub-problems for sub-antenna arrays. After that, the above sub-rate optimization problems are solved separately. The rate of each sub-antenna array is optimized in turn until the last sub-antenna array is optimized. Based on above analysis, the proposed hybrid precoding scheme will be described in detail in the next section.

III. PROPOSED SIC-SVD ALGORITHM

A. DECOMPOSITION OF THE PRECODER DESIGN PROBLEM

Based on the Eq.(6), we design the analog precoding matrix at AP, we first assume that the digital precoding matrix satisfies $\mathbf{F}_{BB}\mathbf{F}_{BB}^H = \mathbf{I}$ to design analog precoder. According to the special sub-connected architecture of analog precoding matrix. We can divide the analog precoding matrix $\mathbf{F}_{RF}$ into $[\mathbf{F}_{RF,N-1}, \mathbf{f}_{RF,N}]$. $\mathbf{f}_{RF,N}$ is the N_{th} column of $\mathbf{F}_{RF}$. $\mathbf{F}_{RF,N-1}$ is a $MN \times (N-1)$ matrix contain the first (N-1) columns of $\mathbf{F}_{RF}$. Then the total achievable rate R in Eq.(6) can be rewritten as:

$$\begin{aligned}\mathrm{R} &= \log_2(|\mathbf{I}_K + \frac{\rho}{N\sigma^2}\mathbf{H}\mathbf{F}_{RF}\mathbf{F}_{RF}^H\mathbf{H}^H|) \\ &= \log_2(|\mathbf{I}_K + \frac{\rho}{N\sigma^2}\mathbf{H}[\mathbf{F}_{RF,N-1}, \mathbf{f}_{RF,N}] \\ &\quad [\mathbf{F}_{RF,N-1}, \mathbf{f}_{RF,N}]^H\mathbf{H}^H|) \\ &= \log_2(|\mathbf{I}_K| + \frac{\rho}{N\sigma^2}\mathbf{H}\mathbf{F}_{RF,N-1}\mathbf{F}_{RF,N-1}^H\mathbf{H}^H \\ &\quad + \frac{\rho}{N\sigma^2}\mathbf{H}\mathbf{f}_{RF,N}\mathbf{f}_{RF,N}^H\mathbf{H}^H)\end{aligned} \tag{10}$$

By defining auxiliary matrix $\mathbf{T}_{N-1}$ as $\mathbf{I}_K + \frac{\rho}{N\sigma^2}\mathbf{H}\mathbf{F}_{RF,N-1}\mathbf{F}_{RF,N-1}^H\mathbf{H}^H$, Eq.(10) can be equivalently expressed as:

$$\begin{aligned}\mathrm{R} &= \log_2(|\mathbf{T}_{N-1}|) \\ &\quad + \log_2(|\mathbf{I}_K + \frac{\rho}{N\sigma^2}\mathbf{T}_{N-1}^{-1}\mathbf{H}\mathbf{f}_{RF,N}\mathbf{f}_{RF,N}^H\mathbf{H}^H|) \\ &\overset{(a)}{=} \log_2(|\mathbf{T}_{N-1}|) \\ &\quad + \log_2(|\mathbf{I}_K + \frac{\rho}{N\sigma^2}\mathbf{f}_{RF,N}^H\mathbf{H}^H\mathbf{T}_{N-1}^{-1}\mathbf{H}\mathbf{f}_{RF,N}|)\end{aligned} \tag{11}$$

and (a) is true due to the fact that $|\mathbf{I} + \mathbf{AB}| = |\mathbf{I} + \mathbf{BA}|$ by defining $\mathbf{A} = \mathbf{T}_{N-1}^{-1}\mathbf{H}\mathbf{f}_{RF,N}$ and $\mathbf{B} = \mathbf{f}_{RF,N}^H\mathbf{H}^H$. The second term on the right side of Eq.(11) represents the achievable sub-rate of the N_{th} sub-antenna array.

Then after N such decompositions, the total achievable rate R in (11) can be presented as:

$$\mathrm{R} = \sum_{n=1}^{N} \log_2(1 + \frac{\rho}{N\sigma^2}\mathbf{f}_{RF,n}^H\mathbf{H}^H\mathbf{T}_{n-1}^{-1}\mathbf{H}\mathbf{f}_{RF,n}) \tag{12}$$

N represents the number of sub-arrays of transmitter. From the transformation of Eq.(10), Eq.(11) and Eq.(12), we observe that the total achievable rate optimization problem can be transformed into a sum of sub-rate optimization problems for a series of sub-antenna array. It can significantly simplify a complex problem that has non-convex constraints. After that, inspired by the SIC method for multi-user signal detection in [28], we can use a similar way to optimize each sub-antenna array sequentially in Fig.3. Then, we present how to design the analog and digital precoding vectors for each sub-antenna array in detail.

Through Eq.(1), it can be seen that the design of hybrid precoding matrix contains analog precoding matrix and digital precoding matrix. Therefore, this paper designs the precoding matrix at the AP in two stages. The analog precoder is designed first, and then design the digital precoder.

B. SIC-BASED ANALOG PRECODER DESIGN

In this section, we focus on how to solve Eq.(12), that is how to design the analog precoding vectors for N sub-antenna arrays. Each sub-antenna array is connected to a RF chain independently, the analog vector of the first sub-antenna array can be optimized by assuming that all the other sub-antenna arrays are closed. From the analysis in Section III-A, it is clear that the sub-rate optimization problem of solving the sub-antenna array analog precoding vector can be described as

$$\mathbf{f}_{RF,n}^{opt} = \arg\max_{\mathbf{f}_{RF,n}\in\mathcal{S}} \log_2(1 + \frac{\rho}{N\sigma^2}\mathbf{f}_{RF,n}^H\mathbf{G}_{n-1}\mathbf{f}_{RF,n}) \tag{13}$$

where $\mathbf{G}_{n-1} = \mathbf{H}^H\mathbf{T}_{n-1}^{-1}\mathbf{H}$, $\mathcal{S}$ is the feasible set of all feasible analog vectors satisfying the constraints proposed in SectionII-B, note that the n_{th} precoding vector only has

M non-zero elements from the $(M(n-1)+1)th$ one to the $(Mn)th$ one. Therefore, the $\mathbf{f}_{RF,n}^H \mathbf{G}_{n-1} \mathbf{f}_{RF,n}$ in Eq.(13) equivalent to $\bar{\mathbf{f}}_{RF,n}^H \overline{\mathbf{G}}_{n-1} \bar{\mathbf{f}}_{RF,n}$. $\bar{\mathbf{f}}_{RF,n}$ denotes the non-zero part of $\mathbf{f}_{RF,n}$. And $\overline{\mathbf{G}}_{n-1} = \mathbf{R}\mathbf{G}_{n-1}\mathbf{R}^H = \mathbf{R}\mathbf{H}^H\mathbf{T}_{n-1}^{-1}\mathbf{H}\mathbf{R}^H$ is the corresponding sub-array matrix of $\mathbf{G}_{n-1}$ by only keeping the rows and columns of $\mathbf{G}_{n-1}$ from the $(M(n-1)+1)th$ one to the $(Mn)th$ one. $\mathbf{R} = [\mathbf{0}_{M\times M(n-1)}\ \mathbf{I}_M\ \ \mathbf{0}_{M\times M(N-n)}]$ is the corresponding selection matrix.

Through the above transformation, the Eq.(13) can be equivalently written as:

$$\bar{\mathbf{f}}_{RF,n}^{opt} = \underset{\bar{\mathbf{f}}_{RF,n}\in\overline{\mathcal{S}}}{\arg\max} \log_2(1 + \frac{\rho}{N\sigma^2} \bar{\mathbf{f}}_{RF,n}^H \overline{\mathbf{G}}_{n-1} \bar{\mathbf{f}}_{RF,n}) \tag{14}$$

$\overline{\mathcal{S}}$ is the feasible set of all possible vectors satisfying *Constraint 2*. After that, we perform SVD operation on the $\overline{\mathbf{G}}_{n-1}$ to obtain $\overline{\mathbf{G}}_{n-1} = \mathbf{V}\Sigma\mathbf{V}^H$, where Σ is a $M \times M$ diagonal matrix containing the singular values of $\overline{\mathbf{G}}_{n-1}$ in a decreasing order, and $\mathbf{V}$ is an $M \times M$ unitary matrix. The optimal unconstrained analog precoding vector $\mathbf{v}_1$ is the first column of $\mathbf{V}$ [29]. If $\bar{\mathbf{f}}_{RF,n} = \mathbf{v}_1$, the system capacity will be maximum. However, due to the constraints mentioned in Section II-B, we cannot choose $\mathbf{v}_1$ as the optimal analog precoding vector directly since elements of $\mathbf{v}_1$ do not obey the constraint of unit modulus amplitude. So we need to choose a suboptimal solution $\bar{\mathbf{f}}_{RF,n}$ as far as possible to near $\mathbf{v}_1$ under the constraint of constant magnitude. From [30], it is known that the optimal analog precoding vector for choosing the optimization problem can be obtained by minimizing the MSE between $\mathbf{v}_1$ and $\bar{\mathbf{f}}_{RF,n}$ under the constant magnitude:

$$\begin{aligned}
&\mathbb{E}\left\|\mathbf{v}_1 - \bar{\mathbf{f}}_{RF,n}\right\|_2^2 \\
&\quad= \mathbb{E}\left\{(\mathbf{v}_1 - \bar{\mathbf{f}}_{RF,n})^H(\mathbf{v}_1 - \bar{\mathbf{f}}_{RF,n})\right\} \\
&\quad= \mathbb{E}\left\{\mathbf{v}_1^H\mathbf{v}_1 + \bar{\mathbf{f}}_{RF,n}^H\bar{\mathbf{f}}_{RF,n} - 2\mathrm{Re}(\mathbf{v}_1^H\bar{\mathbf{f}}_{RF,n})\right\} \\
&\quad\overset{(a)}{=} \mathbb{E}\left\{2 - 2\mathrm{Re}(\mathbf{v}_1^H\bar{\mathbf{f}}_{RF,n})\right\} \\
&\quad= \mathbb{E}\left\{2(1 - \mathrm{Re}(\mathbf{v}_1^H\bar{\mathbf{f}}_{RF,n}))\right\}
\end{aligned} \tag{15}$$

(a) is true due to that $\mathbf{v}_1^H\mathbf{v}_1 = 1, \bar{\mathbf{f}}_{RF,n}^H\bar{\mathbf{f}}_{RF,n} = 1$, according to the above equation, minimizing the MSE is equivalent to selecting an appropriate $\bar{\mathbf{f}}_{RF,n}$ to make the equation (15) equal to 0, since the amplitude of $\bar{\mathbf{f}}_{RF,n}$ is constantly $1/\sqrt{M}$, only the phase is different. From a geometric space perspective, corresponds to the complex plane, different $\bar{\mathbf{f}}_{RF,n}$ are located on circle with the same radius. Obviously, the distance between points with the same phase is the closest, and each element of $\bar{\mathbf{f}}_{RF,n}$ has the same amplitude $1/\sqrt{M}$. Thus the analog precoding vector is obtained from the extracted phase as:

$$\mathbf{f}_{RF,n}^{opt} = \frac{1}{\sqrt{M}} e^{j\angle\mathbf{v}_1} \tag{16}$$

$\angle\mathbf{v}_1$ denotes the phase of vector $\mathbf{v}_1$. After we have acquired $\bar{\mathbf{f}}_{RF,n}$ for the *nth* sub-antenna array, the auxiliary matrix $\mathbf{T}_n$ and $\overline{\mathbf{G}}_n$ will be updated. The remaining several sub-antenna array are designed by: updated $\overline{\mathbf{G}}_n$ and SVD is performed to obtain the optimal analog precoder vectors for other sub-antenna arrays. Then we can obtain the optimal analog precoding matrix:

$$\mathbf{F}_{RF}^{opt} = diag\left\{\mathbf{f}_{RF,1}^{opt}, \mathbf{f}_{RF,2}^{opt}, \ldots, \mathbf{f}_{RF,N}^{opt}\right\} \tag{17}$$

C. DESIGN OF DIGITAL PRECODER BASED ON EQUIVALENT CHANNEL

After the design of analog precoders for all sub-antenna arrays at AP are completed. We fix the analog precoding matrix, then pay attention to design the digital precoding matrix.

In this section, we introduce the concept of equivalent channel [31], [32], [33], i.e. define $\mathbf{H}_{eq} = \mathbf{H}\mathbf{F}_{RF}$ as the equivalent channel matrix at the baseband. After that, we will design digital precoding vectors based on the equivalent channel matrix $\mathbf{H}_{eq} \in \mathbb{C}^{N_r\times N}$ to further promote system sum rate performance. We bring the equivalent channel into Eq.(6) to get:

$$\mathrm{R} = \log_2(|\mathbf{I}_K + \frac{\rho}{N\sigma^2}\mathbf{H}_{eq}\mathbf{F}_{BB}\mathbf{F}_{BB}^H\mathbf{H}_{eq}^H|) \tag{18}$$

In order to maximize the achievable rate of this communication system, finding the digital precoding matrix is equivalent to:

$$\mathbf{F}_{BB}^{opt} = \arg\max \log_2(|\mathbf{I}_K + \frac{\rho}{N\sigma^2}\mathbf{H}_{eq}\mathbf{F}_{BB}\mathbf{F}_{BB}^H\mathbf{H}_{eq}^H|) \tag{19}$$

The common digital precoding techniques include: ZF precoding, MMSE precoding, BD precoding, etc. SVD precoding is a technique used for channel precoding in multi-antenna wireless communication systems. In order to avoid multiple operations and obtain better performance, the transmission power constraints of AP will not be considered temporarily, the SVD operation is applied to the equivalent channel matrix $\mathbf{H}_{eq}$ to design optimal digital matrix [34]:

$$\mathbf{H}_{eq} = \mathbf{U}_{eq}\Sigma_{eq}\mathbf{V}_{eq}^H \tag{20}$$

where $\mathbf{U}_{eq} \in \mathbb{C}^{N_r\times N}$ and $\mathbf{V}_{eq}^H \in \mathbb{C}^{N\times N}$ are left and right singular matrices of the equivalent channel matrix, respectively, and both are unitary matrices. $\Sigma_{eq} \in \mathbb{C}^{N\times N}$ is a diagonal matrix, which represents singular value matrix of the equivalent channel. SVD precoding can fully utilize the channel, decompose it into multiple orthogonal and no-interference sub-channels for signal transmission, eliminate the mutual influence between data streams.

For the convenience of further design the digital precoding matrix, performing a simple transformation on Eq.(18):

$$R = \log_2(|\mathbf{I}_K + \frac{\rho}{N\sigma^2}\mathbf{F}_{BB}^H\mathbf{H}_{eq}^H\mathbf{H}_{eq}\mathbf{F}_{BB}|) \tag{21}$$

Taking the decomposed result Eq.(20) into Eq.(21) we can get:

$$\begin{aligned}
\mathrm{R} &= \log_2(|\mathbf{I}_K + \frac{\rho}{N\sigma^2}\mathbf{F}_{BB}^H\mathbf{H}_{eq}^H\mathbf{H}_{eq}\mathbf{F}_{BB}|) \\
&= \log_2(|\mathbf{I}_K + \frac{\rho}{N\sigma^2}\mathbf{F}_{BB}^H\mathbf{V}_{eq}\Sigma_{eq}^H\mathbf{U}_{eq}^H\mathbf{U}_{eq}\Sigma_{eq}\mathbf{V}_{eq}^H\mathbf{F}_{BB}|)
\end{aligned}$$

$$\stackrel{(a)}{=} \log_2(|\mathbf{I}_K + \frac{\rho}{N\sigma^2}\mathbf{F}_{BB}^H\mathbf{V}_{eq}\Sigma_{eq}^2\mathbf{V}_{eq}^H\mathbf{F}_{BB}|) \quad (22)$$

(a) is true due to the fact that $\mathbf{U}_{eq}\mathbf{U}_{eq}^H = \mathbf{I}$. By observing the above equation and utilizing the properties of unitary matrix, to maximize Eq.(22), the optimal digital precoding solution $\mathbf{F}_{BB}^{opt}$ of $\mathbf{F}_{BB}$ is $\mathbf{V}_{eq}$. In addition, due to the fact that the number of RF chains at AP equal to N, same dimension as matrix $\mathbf{V}$. So we can get optimal digital precoding matrix $\mathbf{F}_{BB}$ at AP is:

$$\mathbf{F}_{BB}^{opt} = \mathbf{V}_{eq} = [\mathbf{V}_{eq,1}, \mathbf{V}_{eq,2}, \cdots, \mathbf{V}_{eq,N}] \quad (23)$$

Up to now, the design of analog/digital precoding matrix has been wholly completed. In general, the specific steps of the proposed SIC-SVD hybrid precoding algorithm in this article can be simply summarized as follows:

step 1:Input: Channel matrix $\mathbf{H}$
Number of RF chains: N_t^{RF}
Number of antennas in a sub-antenna array: M
step 2:Obtain matrix:
$\overline{\mathbf{G}}_{n-1} = \mathbf{R}\mathbf{G}_{n-1}\mathbf{R}^H = \mathbf{R}\mathbf{F}^H\mathbf{T}_{n-1}^{-1}\mathbf{H}\mathbf{R}^H$
step 3:Execute the SVD of obtained matrix $\overline{\mathbf{G}}_{n-1}$ to obtain $\mathbf{v}_1$
step 4:Analog precoding vector:
$\mathbf{f}_{RF,n}^{opt} = \frac{1}{\sqrt{M}}e^{j\angle\mathbf{v}_1}$
step 5:Update the matrix of n_{th} sub-array
$\overline{\mathbf{G}}_{n-1} = \mathbf{R}\mathbf{H}^H\mathbf{T}_n^{-1}\mathbf{H}\mathbf{R}^H$
and $\mathbf{T}_n = \mathbf{I}_K + \frac{\rho}{N\sigma^2}\mathbf{H}\mathbf{F}_{RF,n}\mathbf{F}_{RF,n}^H\mathbf{H}^H$
Repeat step 1-5 for the *Nth* sub-array at AP.
step 6: Obtain equivalent channel matrix based on the design analog precoding matrix: $\mathbf{H}_{eq} = \mathbf{H}\mathbf{F}_{RF}$.
step 7: Execute the SVD of equivalent channel matrix:
$\mathbf{H}_{eq} = \mathbf{U}_{eq}\Sigma_{eq}\mathbf{V}_{eq}^H$
step 8:Digital precoding matrix:
$\mathbf{F}_{BB} = \mathbf{V}_{eq}(:, 1 : N_t^{RF})$
step 9:Output: Precoding matrix:$\mathbf{F}_{RF}$, $\mathbf{F}_{BB}$

IV. SIMULATION RESULTS

In this section, we provide simulation results for achievable rate of the system. In order to better compare the performance of proposed SIC-SVD hybrid precoding method, simulation results provide the system achievable rate under different SNRs, the SIC-based hybrid precoding with sub-connected architecture and the optimal unconstrained precoding methods based on fully-connected and sub-connected structures ($\overline{\mathbf{f}}_n^{opt} = \mathbf{v}_1$) and conventional analog precoding method [35] are also compared and analysed.

The system simulation parameters are set as follows. The carrier frequency is set as 0.28 THz, $NM \times K = 128/256 \times 16$, NM represents the total number of antennas at AP. K represents the number of antennas at user, N reprents the numbers of RF chain and data stream,($K = N$). The number of effective channel path L is set as 3. The antenna arrays at AP and user are both ULAs. The channel matrix is generated according to the channel model described in Section.II Eq.(4), with the spacing between the antennas set to $d = \lambda/2$. The AoDs at AP satisfy $[-\pi,\pi]$ uniform distribution. The AoAs satisfy $[-\pi/6, \pi/6]$ distribution. The simulation results are obtained by averaging 10000 experiments on the channel using the Monte Carlo method.

We first evaluate the achievable rate with different hybrid precoding design methods. In the analysis process of this section, we assume that the channel has perfect CSI condition. Fig.4 shows the achievable rate in indoor Sub-THz point-to-point system, where $MN \times K = 128 \times 16(M = 8)$ and the number of RF chains N is 16. We observe from Fig.4 that the proposed hybrid SIC-SVD precoding outperforms the conventional analog precoding with sub-connected architecture over the whole simulated SNR region. The performance is also slightly better than the SIC hybrid precoding method. In addition, the proposed SIC-SVD algorithm in this simulation parameters is very close to the optimal unconstrained precoding using sub-connected architecture.

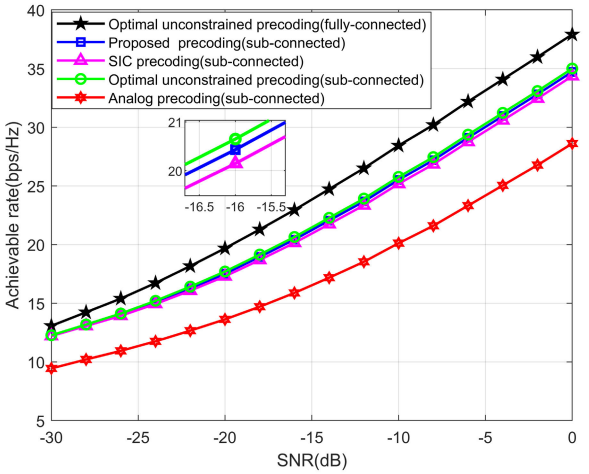

FIGURE 4. Achievable rate comparison for an $NM \times K = 128 \times 16$(N=16) Sub-THz system.

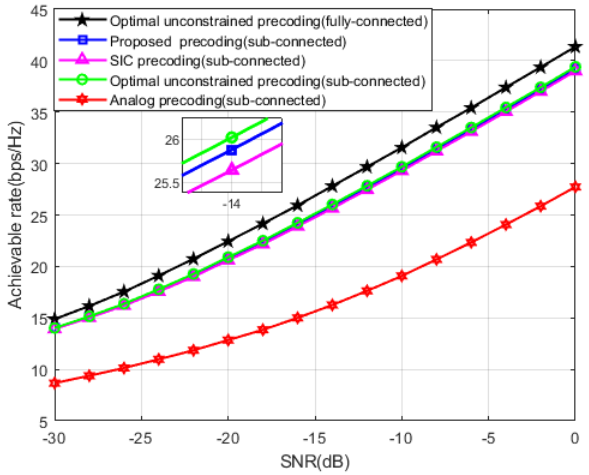

FIGURE 5. Achievable rate comparison for an $NM \times K = 128 \times 32$(N=32) Sub-THz system.

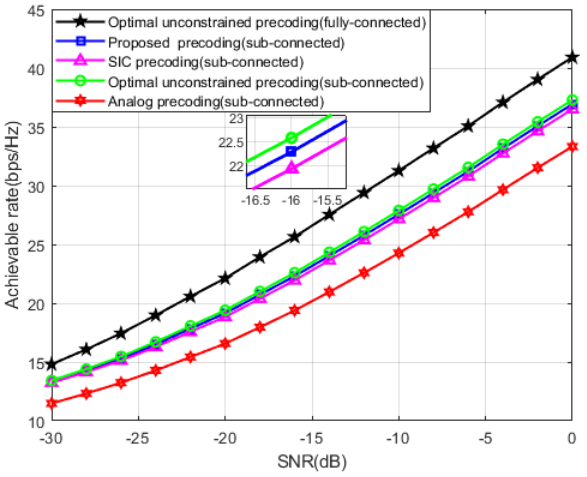

FIGURE 6. Achievable rate comparison for an $NM \times K$=256 × 16(N=16) Sub-THz system.

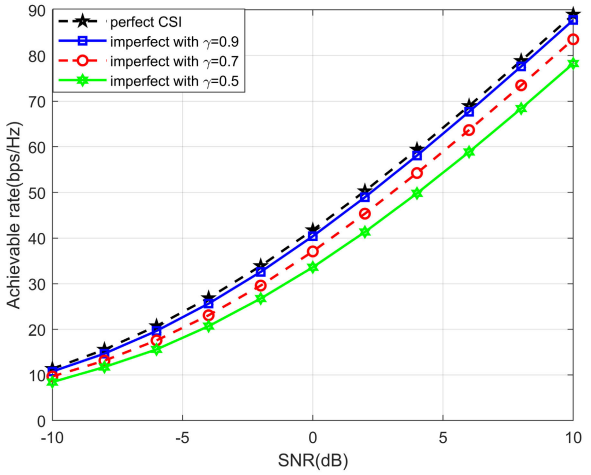

FIGURE 7. Impact of imperfect CSI on the proposed SIC-SVD precoding for 128× 16(N=16) Sub-THz system.

Based on the above simulation results, we will compare again by changing the number of RF chains at AP. Fig.5 shows the simulation results after changing the RF chains from 16 to 32. By observing and comparing Fig.4 and Fig.5, we can easily find that the proposed SIC-SVD method can still keep good and steady performance even with an increase in the number of RF chains. In addition, we can also conclude that as the number of RF chains increases, the system's achievable rate also improves. Such as, when SNR = 0 dB, the RF chains N=16, the achievable rate of the proposed SIC-SVD method is 21.53 bps/Hz, when SNR = 0dB, the RF chains N=32, the achievable rate of the proposed SIC-SVD method is 25.97 bps/Hz.

Fig.6 also shows the relationship between the system achievable rate and different SNRs for the algorithms such as the proposed hybrid SIC-SVD precoding method and the optimal precoding methods with sub-connected while $MN \times K = 256 \times 16(N = 16)$ and the antenna array structures at AP and user are both ULAs. From the simulation results, although the number of antennas at AP has increased, it can be seen that the achievable rate of different algorithms are still increase with the increase of SNRs. The algorithm proposed in this paper is very close to the optimal precoding in terms of performance effective and is better than the precoding method based on SIC [16]. From Fig.4, Fig.5 and Fig.6, we can observe that the proposed algorithm maintains good performance regardless of variations in the number of transmit antennas or RF chains. The channel information plays a crucial role in the design of precoding techniques. In this paper, the proposed algorithm considers the channel information by utilizing an equivalent channel matrix that incorporates both channel matrix and analog precoding matrix. The algorithm takes advantage of the channel information and employed SVD to obtain the optimal digital precoding matrix. As a result, the proposed algorithm outperforms other existing algorithms in terms of performance.

Next we analyze a more practical scenario where AP has imperfect CSI, and evaluate the impact of imperfect CSI on the performance of the proposed SIC-SVD precoding algorithm. In the previous simulation of this paper, we all assume perfect CSI at AP and receiver. However, in practical communication environments, we sometimes cannot obtain perfect CSI due to uncertainties in the transmission environment and other factors such as estimation, feedback delays, etc which will introduce errors [36]. No matter how precisely or accurately design the channel estimation algorithms, there will always be an error between the estimated channel and the actual channel. Therefore, it is necessary to consider the impact of imperfect CSI on the performance of the proposed algorithm. The estimated channel matrix for the channel state information $\hat{\mathbf{H}}$ can be modeled as follows [37]:

$$\hat{\mathbf{H}} = \gamma \mathbf{H} + \sqrt{1-\gamma^2}\mathbf{E} \tag{24}$$

In the expression, $\mathbf{H}$ represents the actual channel matrix, $\gamma \in [0, 1]$ represents the estimated CSI accuracy, and $\mathbf{E}$ is the error matrix that follows the distribution i.i.d. $\mathcal{CN}(0, 1)$.

Fig.7 shows achievable rate comparison for the system with $MN \times K = 128 \times 16(N = 16)$, considering both perfect CSI and imperfect CSI with different values of γ. The simulation results indicate that the proposed SIC-SVD method is not very sensitive to the accuracy of the channel state information. In Fig.7, achievable rate of the proposed SIC-SVD hybrid precoding method with γ=0.9 is very near to the perfect CSI, and even the channel state information is very poor (γ=0.5), the performance of the proposed SIC-SVD hybrid precoding method does not decrease significantly and a relatively high rate can still be achieved. Additionally, Fig.8 shows the achievable rate comparison for a indoor Sub-THz system with $MN \times K = 256 \times 16(N = 16)$, where similar conclusions as those from Fig.8 can be derived. It is worth noting that in Fig.8, the performance with γ=0.9 almost overlaps with the performance with perfect CSI. By observing

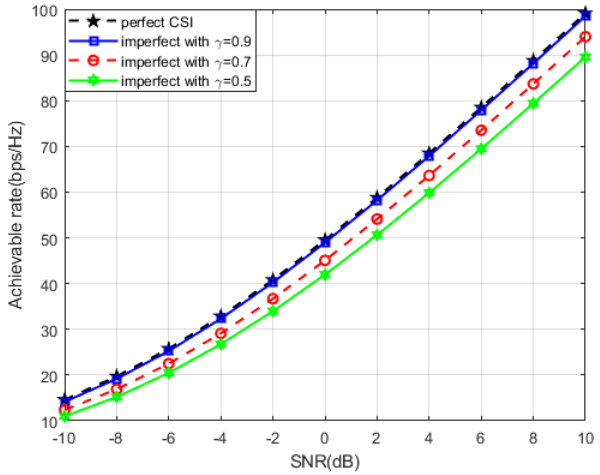

FIGURE 8. Impact of imperfect CSI on the proposed SIC-SVD precoding for 256× 16(N=16) Sub-THz system.

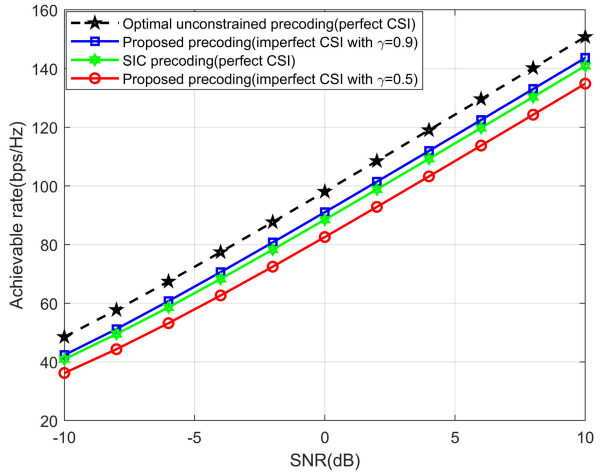

FIGURE 9. Achievable rate by different algorithms under the perfect CSI and imperfect CSI for 256× 16(N=16) Sub-THz system.

Fig.7 and Fig.8, it can be demonstrated that the proposed SIC-SVD method has strong robustness and stability.

Fig.9 shows the performance comparison between different algorithms (i.e. optimal unconstrained precoding, SIC precoding) under perfect CSI conditions and the proposed SIC-SVD precoding algorithm under imperfect CSI conditions. The algorithms in Fig.9 are all simulated under sub-connected architecture. Comparing the experimental results of different algorithms, it is not difficult to find that when $\gamma = 0.9$, performance of the proposed SIC-SVD algorithms are still superior to the SIC precoding algorithm. The performance of SIC algorithm lies between the estimated CSI accuracy γ is 0.9 and 0.5, respectively.

V. CONCLUSION

In this paper, an improved hybrid precoding method is proposed for a simple indoor communication system based on sub-connected structures in sub-THz band. Using the idea of SIC, the complex rate optimization problem is decomposed into a series of sub-rate optimization problems, the digital precoding matrix is first fixed to design the analog precoding using SIC method, then the digital precoding part is designed using conventional SVD precoding method based on the equivalent channel. Simulation results also show that the performance of the proposed algorithm is close to the achievable rate of optimal unconstrained precoding. The scheme uses sub-connected structure, which effectively reduces the complexity of signal processing and approached the performance of the optimal precoding. We also compared the performance of proposed algorithm with different accuracy CSI. Our future work can be extended to the multi-user scenarios.

ACKNOWLEDGMENT

The author would like to thank the support of the National Science Foundation of China and the National Science Foundation of Hunan Province.

REFERENCES

[1] I. F. Akyildiz, A. Kak, and S. Nie, "6G and beyond: The future of wireless communications systems," *IEEE Access*, vol. 8, pp. 133995–134030, 2020.

[2] J. G. Andrews, S. Buzzi, W. Choi, S. V. Hanly, A. Lozano, A. C. K. Soong, and J. C. Zhang, "What will 5G be?" *IEEE J. Sel. Areas Commun.*, vol. 32, no. 6, pp. 1065–1082, Jun. 2014.

[3] H.-J. Song and T. Nagatsuma, "Present and future of terahertz communications," *IEEE Trans. THz Sci. Technol.*, vol. 1, no. 1, pp. 256–263, Sep. 2011.

[4] I. F. Akyildiz, J. M. Jornet, and C. Han, "Terahertz band: Next frontier for wireless communications," *Phys. Commun.*, vol. 12, pp. 16–32, Sep. 2014.

[5] J. Tan and L. Dai, "THz precoding for 6G: Challenges, solutions, and opportunities," *IEEE Wireless Commun.*, early access, May 9, 2022, doi: 10.1109/MWC.015.2100674.

[6] B. Ning, Z. Tian, W. Mei, Z. Chen, C. Han, S. Li, J. Yuan, and R. Zhang, "Beamforming technologies for ultra-massive MIMO in terahertz communications," *IEEE Open J. Commun. Soc.*, vol. 4, pp. 614–658, 2023.

[7] P. Yang, Y. Xiao, M. Xiao, and S. Li, "6G wireless communications: Vision and potential techniques," *IEEE Netw.*, vol. 33, no. 4, pp. 70–75, Jul. 2019.

[8] C. Lin and G. Y. Li, "Indoor terahertz communications: How many antenna arrays are needed?" *IEEE Trans. Wireless Commun.*, vol. 14, no. 6, pp. 3097–3107, Jun. 2015.

[9] C. Lin and G. Y. Li, "Energy-efficient design of indoor mmWave and sub-THz systems with antenna arrays," *IEEE Trans. Wireless Commun.*, vol. 15, no. 7, pp. 4660–4672, Jul. 2016.

[10] S. Priebe and T. Kurner, "Stochastic modeling of THz indoor radio channels," *IEEE Trans. Wireless Commun.*, vol. 12, no. 9, pp. 4445–4455, Sep. 2013.

[11] H. Sarieddeen, M.-S. Alouini, and T. Y. Al-Naffouri, "An overview of signal processing techniques for terahertz communications," *Proc. IEEE*, vol. 109, no. 10, pp. 1628–1665, Oct. 2021.

[12] S. Han, I. Chih-Lin, Z. Xu, and C. Rowell, "Large-scale antenna systems with hybrid analog and digital beamforming for millimeter wave 5G," *IEEE Commun. Mag.*, vol. 53, no. 1, pp. 186–194, Jan. 2015.

[13] C. Rusu, R. Méndez-Rial, N. González-Prelcicy, and R. W. Heath Jr., "Low complexity hybrid sparse precoding and combining in millimeter wave MIMO systems," in *Proc. IEEE Int. Conf. Commun. (ICC)*, London, U.K., Jun. 2015, pp. 1340–1345.

[14] L. Liang, W. Xu, and X. Dong, "Low-complexity hybrid precoding in massive multiuser MIMO systems," *IEEE Wireless Commun. Lett.*, vol. 3, no. 6, pp. 653–656, Dec. 2014.

[15] C. Lin and G. Y. L. Li, "Terahertz communications: An array-of-subarrays solution," *IEEE Commun. Mag.*, vol. 54, no. 12, pp. 124–131, Dec. 2016.

[16] X. Gao, L. Dai, S. Han, I. Chih-Lin, and R. W. Heath Jr., "Energy-efficient hybrid analog and digital precoding for mmWave MIMO systems with large antenna arrays," *IEEE J. Sel. Areas Commun.*, vol. 34, no. 4, pp. 998–1009, Apr. 2016.

[17] Y. Liu, Q. Feng, Q. Wu, Y. Zhang, M. Jin, and T. Qiu, "Energy-efficient hybrid precoding with low complexity for mmWave massive MIMO systems," *IEEE Access*, vol. 7, pp. 95021–95032, 2019.
[18] S. Hur, T. Kim, D. J. Love, J. V. Krogmeier, T. A. Thomas, and A. Ghosh, "Millimeter wave beamforming for wireless backhaul and access in small cell networks," *IEEE Trans. Commun.*, vol. 61, no. 10, pp. 4391–4403, Oct. 2013.
[19] M. Zhu, G. Xie, and X. Qi, "Low-complexity partially-connected hybrid precoding for massive MIMO systems," in *Proc. IEEE Wireless Commun. Netw. Conf. (WCNC)*, Seoul, South Korea, May 2020, pp. 1–6.
[20] L. Yan, C. Han, and J. Yuan, "A dynamic array-of-subarrays architecture and hybrid precoding algorithms for terahertz wireless communications," *IEEE J. Sel. Areas Commun.*, vol. 38, no. 9, pp. 2041–2056, Sep. 2020.
[21] T. E. Bogale and L. B. Le, "Massive MIMO and mmWave for 5G wireless HetNet: Potential benefits and challenges," *IEEE Veh. Technol. Mag.*, vol. 11, no. 1, pp. 64–75, Mar. 2016.
[22] C. Han, A. O. Bicen, and I. F. Akyildiz, "Multi-ray channel modeling and wideband characterization for wireless communications in the terahertz band," *IEEE Trans. Wireless Commun.*, vol. 14, no. 5, pp. 2402–2412, May 2015.
[23] Y. Zhang, D. Li, D. Qiao, and L. Zhang, "Analysis of indoor THz communication systems with finite-bit DACs and ADCs," *IEEE Trans. Veh. Technol.*, vol. 71, no. 1, pp. 375–390, Jan. 2022.
[24] D. Li, D. Qiao, L. Zhang, and G. Y. Li, "Performance analysis of indoor THz communications with one-bit precoding," in *Proc. IEEE Global Commun. Conf. (GLOBECOM)*, Abu Dhabi, United Arab Emirates, Dec. 2018, pp. 1–7.
[25] X. Xu, R. Zhang, and Y. Qian, "Location-based hybrid precoding schemes and QoS-aware power allocation for radar-aided UAV–UGV cooperative systems," *IEEE Access*, vol. 10, pp. 50947–50958, 2022.
[26] C. A. Balanis, *Antenna Theory: Analysis and Design*. Hoboken, NJ, USA: Wiley, 2015.
[27] R. Méndez-Rial, C. Rusu, N. González-Prelcic, A. Alkhateeb, and R. W. Heath Jr., "Hybrid MIMO architectures for millimeter wave communications: Phase shifters or switches?" *IEEE Access*, vol. 4, pp. 247–267, 2016.
[28] Y.-C. Liang, E. Y. Cheu, L. Bai, and G. Pan, "On the relationship between MMSE-SIC and BI-GDFE receivers for large multiple-input multiple-output channels," *IEEE Trans. Signal Process.*, vol. 56, no. 8, pp. 3627–3637, Aug. 2008.
[29] O. E. Ayach, S. Rajagopal, S. Abu-Surra, Z. Pi, and R. W. Heath Jr., "Spatially sparse precoding in millimeter wave MIMO systems," *IEEE Trans. Wireless Commun.*, vol. 13, no. 3, pp. 1499–1513, Mar. 2014.
[30] L. Dai, X. Gao, J. Quan, S. Han, and I. Chih-Lin, "Near-optimal hybrid analog and digital precoding for downlink mmWave massive MIMO systems," in *Proc. IEEE Int. Conf. Commun. (ICC)*, London, U.K., Jun. 2015, pp. 1334–1339.
[31] M. Cui and W. Zou, "Low complexity joint hybrid precoding for millimeter wave MIMO systems," *China Commun.*, vol. 16, no. 2, pp. 49–58, Feb. 2019.
[32] S. Zhou, W. Xu, H. Zhang, and X. You, "Hybrid precoding for millimeter wave massive MIMO with analog combining," in *Proc. 9th Int. Conf. Wireless Commun. Signal Process. (WCSP)*, Nanjing, China, Oct. 2017, pp. 1–5.
[33] S. Wang, Z. Li, M. He, T. Jiang, R. Ruby, H. Ji, and V. C. M. Leung, "A joint hybrid precoding/combining scheme based on equivalent channel for massive MIMO systems," *IEEE J. Sel. Areas Commun.*, vol. 40, no. 10, pp. 2882–2893, Oct. 2022.
[34] A. Li and C. Masouros, "Hybrid precoding and combining design for millimeter-wave multi-user MIMO based on SVD," in *Proc. IEEE Int. Conf. Commun. (ICC)*, Paris, France, May 2017, pp. 1–6.
[35] O. El Ayach, R. W. Heath Jr., S. Rajagopal, and Z. Pi, "Multimode precoding in millimeter wave MIMO transmitters with multiple antenna subarrays," in *Proc. IEEE Global Commun. Conf. (GLOBECOM)*, Atlanta, GA, USA, Dec. 2013, pp. 3476–3480.
[36] D. Jagyasi and P. Ubaidulla, "Low-complexity transceiver design for multi-user millimeter wave communication systems under imperfect CSI," in *Proc. IEEE 84th Veh. Technol. Conf. (VTC-Fall)*, Montreal, QC, Canada, Sep. 2016, pp. 1–5.
[37] F. Rusek, D. Persson, B. K. Lau, E. G. Larsson, T. L. Marzetta, and F. Tufvesson, "Scaling up MIMO: Opportunities and challenges with very large arrays," *IEEE Signal Process. Mag.*, vol. 30, no. 1, pp. 40–60, Jan. 2013.

HANG GUI received the B.S. degree in communication engineering from Huanghuai University, Zhumadian, China, in 2021. He is currently pursuing the master's degree in electronic information with Jishou University. His research interests include hybrid precoding array signal processing and wireless communications.

YUANYUAN XIE received the B.S. degree in information engineering from East China Jiaotong University, Nanchang, China, in 2022. She is currently pursuing the master's degree in electronic information with Jishou University. Her research interests include hybrid precoding, array signal processing, and MIMO communications.

QINGHENG SONG received the B.S. degree in electronic information engineering from the Guilin University of Technology, Guilin, China, in 2003, the M.S. degree from the Huazhong University of Science and Technology, Wuhan, China, in 2009, and the Ph.D. degree in information and communication engineering from the National Mobile Communication Research Laboratory, Southeast University, Nanjing, China, in 2019. He has been an Associate Professor of physics of electrical and intelligent manufacturing with Huaihua University. His research interests include UAV communications and MIMO communications.

YINGJING QIAN received the B.S. degree in communications engineering from Nanchang University, Nanchang, China, in 2004, and the M.S. degree in circuits and systems from Hunan University, Changsha, China, in 2011. She is currently an Associate Professor with the College of Electrical and Information Engineering, Huaihua University. Her research interests include wireless communications and machine learning.

RENMIN ZHANG (Member, IEEE) received the B.S. degree in electronic engineering from the Guilin University of Electronic Technology, Guilin, China, in 2003, the M.S. degree in electronic and communication engineering from Peking University, Beijing, China, in 2011, and the Ph.D. degree in information and communication engineering from Southeast University, Nanjing, China, in 2019. He is currently a Professor with the School of Communication and Electronic Engineering, Jishou University. His research interests include MIMO communications, signal processing, and THz communications.